



UNIVERSIDADE ESTADUAL DE CAMPINAS
SISTEMA DE BIBLIOTECAS DA UNICAMP
REPOSITÓRIO DA PRODUÇÃO CIENTÍFICA E INTELLECTUAL DA UNICAMP

Versão do arquivo anexado / Version of attached file:

Versão do Editor / Published Version

Mais informações no site da editora / Further information on publisher's website:

<https://opg.optica.org/oe/fulltext.cfm?uri=oe-19-3-1936&id=209598>

DOI: 10.1364/OE.19.001936

Direitos autorais / Publisher's copyright statement:

©2011 by Optical Society of America. All rights reserved.

DIRETORIA DE TRATAMENTO DA INFORMAÇÃO

Cidade Universitária Zeferino Vaz Barão Geraldo

CEP 13083-970 – Campinas SP

Fone: (19) 3521-6493

<http://www.repositorio.unicamp.br>

Electromagnetically-induced phase grating: A coupled-wave theory analysis

Silvânia A. Carvalho and Luís E. E. de Araujo*

Instituto de Física "Gleb Wataghin," Universidade Estadual de Campinas, Campinas - SP,
13083-859, Brazil

araujo@ifi.unicamp.br

Abstract: We use a coupled-wave theory analysis to describe an atomic phase grating based on the giant Kerr nonlinearity of an atomic medium under electromagnetically induced transparency. An analytical expression is found for the diffraction efficiency of the grating. Efficiencies greater than 70% are predicted for incidence at the Bragg angle.

© 2011 Optical Society of America

OCIS codes: (020.1670) Atomic and molecular physics; (270.1670) Quantum optics; (050.2770) Diffraction and gratings

References and links

1. M. Fleischhauer, A. Imamoglu A and J. P. Marangos, "Electromagnetically induced transparency: Optics in coherent media," *Rev. Mod. Phys.* **77**, 633-673 (2005).
2. A. W. Brown and M. Xiao, "All-optical switching and routing based on an electromagnetically induced absorption grating," *Opt. Lett.* **30**, 699-701 (2005).
3. M. Bajcsy, A. S. Zibrov, and M. D. Lukin, "Stationary pulses of light in an atomic medium," *Nature* **426**, 638-641 (2003).
4. D. Moretti, D. Felinto, J. W. R. Tabosa, and A. Lezama, "Dynamics of a stored Zeeman coherence grating in an external magnetic field," *J. Phys. B* **43**, 115502 (2010).
5. H. Y. Ling, Y.-Q. Li and M. Xiao, "Electromagnetically induced grating: Homogeneously broadened medium," *Phys. Rev. A* **57**, 1338-1344 (1998).
6. M. Mitsunaga and N. Imoto, "Observation of an electromagnetically induced grating in cold sodium atoms," *Phys. Rev. A* **59**, 4773-4776 (1990).
7. G. C. Cardoso and J. W. R. Tabosa, "Electromagnetically induced gratings in a degenerate open two-level system," *Phys. Rev. A* **65**, 033803 (2002).
8. J. W. Goodman, *Introduction to Fourier Optics* (McGraw-Hill, New York, 1968).
9. L. E. E. de Araujo, "Electromagnetically induced phase grating," *Opt. Lett.* **35**, 977-979 (2010).
10. H. Schmidt and A. Imamoglu, "Giant Kerr nonlinearities obtained by electromagnetically induced transparency," *Opt. Lett.* **21**, 1936-1938 (1996).
11. Z.-H. Xiao, S. G. Shin and K. Kim, "An electromagnetically induced grating by microwave modulation," *J. Phys. B* **43**, 161004 (2010).
12. L. Zhao, W. Duan, and S. F. Yelin, "All-optical beam control with high speed using image-induced blazed gratings in coherent media," *Phys. Rev. A* **82**, 013809 (2010).
13. W. R. Klein and B. D. Cook, "Unified approach to ultrasonic light diffraction," *Trans. Sonics Ultrason.* **SU14**, 123 (1967).
14. H. Kogelnik, "Coupled wave theory for thick hologram gratings," *Bell Syst. Tech. J.* **48**, 2909-2947 (1969).
15. H. S. Kang and Y. F. Zhu, "Observation of Large Kerr Nonlinearity at Low Light Intensities," *Phys. Rev. Lett.* **91**, 093601 (2003).
16. W. Ketterle, K. B. Davis, M. A. Joffe, A. Martin, and D. E. Pritchard, "High densities of cold atoms in a dark spontaneous-force optical trap," *Phys. Rev. Lett.* **70**, 2253-2256 (1993).
17. S. Magkiriadou, D. Patterson, T. Nicolas and J. M. Doyle, "Cold, Optically Dense Gases of Atomic Rubidium," <http://www.doylegroup.harvard.edu/wiki/index.php/Publications>.

1. Introduction

An electromagnetically induced grating (EIG) can diffract a probe beam into high order directions. An EIG is formed when a standing wave pattern is imprinted on an atomic sample, modulating the absorption or index of refraction of the atoms. In the former, the EIG is an amplitude grating, and in the latter, a phase grating. In either case, the main physical phenomenon responsible for the grating is electromagnetically induced transparency (EIT) [1]. Under EIT, an atomic medium becomes transparent to a resonant probe field by means of a stronger coupling field acting on a linked transition. The atom also experiences a very steep dispersion near resonance. Electromagnetically induced gratings find applications in all optical switching and routing [2] and light storage [3, 4].

An atomic absorption grating was theoretically proposed for the first time in [5] and then experimentally demonstrated in cold [6, 7] and hot [2] atomic samples. In an electromagnetically-induced absorption grating, alternating regions of high transmission and absorption are created in the atomic sample, which act as an amplitude grating. Amplitude gratings in general are well known for having a low diffraction power, as opposed to a phase grating, which disperses energy into higher diffraction orders much more efficiently [8]. A phase modulation can be added to an atomic amplitude grating by detuning the probe field away from resonance, thus creating a mixed grating [5].

For high diffraction efficiency, an ideal phase grating should, however, consist of a medium that is completely transparent to the probe beam, but capable of imparting a π phase shift across the probe beam. An atomic phase grating, based on cross phase modulation (XPM) of the probe beam, was recently proposed by one of the authors [9]. By modulating the giant Kerr nonlinearity the atomic medium experiences under EIT [10], the grating of Ref. [9] imparts a π phase modulation to the probe field while simultaneously maintains a high probe transmission. This phase grating was shown to diffract light efficiently, approaching the performance of an ideal sinusoidal phase grating [8]. Furthermore, the phase grating can be created with weak fields, possibly finding application in all-optical switching at low light levels. Alternatively, a phase grating can also be induced in an atomic sample by modulating a weak microwave field applied to a double dark-state system [11] or by using intensity-modulated images to create a blazed transmission grating [12].

In the work described in [9], the atomic grating was treated in the Raman-Nath regime with the probe beam entering the grating at normal incidence and producing several diffracted waves. Diffraction efficiencies approaching 30% into the ± 1 orders were predicted for a grating thickness $\ell \approx 160z_0$, where $z_0 = \hbar\epsilon_0\lambda\gamma_c/4\pi N\mu_{ac}^2$ is the linear absorption length in the absence of EIT; N is the atomic density, μ_{ac} is the electric dipole moment, and γ_c is the natural linewidth of the atomic transition. For $N = 10^{18} \text{ m}^{-3}$, $\mu_{ac} = 2.49 \times 10^{-29} \text{ Cm}$ and $\gamma_c = 2\pi \times 9.8 \text{ MHz}$, then $\ell \approx 2 \text{ mm}$, which is three orders of magnitude larger than the grating period $\Lambda \approx 2 \mu\text{m}$ for a probe wavelength $\lambda = 589 \text{ nm}$, suggesting the grating is thick.

In the holographic and acoustic grating literature, a grating is considered thick if the parameter Q of Klein and Cook [13], defined as $Q = 2\pi\lambda\ell/\Lambda^2$, is greater than 10. In the atomic grating of Ref. [9], $Q \approx 1850$. Therefore, that grating, in fact, can be considered thick. It should show Bragg behavior and produce only one diffracted beam for Bragg angle incidence. Therefore, even higher diffraction efficiencies than originally predicted in Ref. [9] should become possible if the Bragg phase-matching condition is satisfied. Propagation of the incident and diffracted light fields inside a thick grating, in the Bragg regime, is best described in terms of a coupled wave analysis [14].

In this paper, we study the atomic phase grating described in Ref. [9] in light of coupled wave theory. We derive an analytical expression for the diffraction efficiency of the grating and study how the efficiency depends on the excitation parameters. To the best of our knowledge, this

is the first time coupled wave theory is applied to describe an EIG. The paper is organized as follows. In section 2 we discuss the atomic model for creating an electromagnetically-induced phase grating. In section 3, we apply the coupled wave analysis to the atomic phase grating. We present our results and discussion in section 4. Section 5 concludes the paper.

2. Atomic model for an electromagnetically-induced phase grating

Figure 1a illustrates the atomic model. It consists of a type N four-level atom being driven by three cw lasers. Levels $|c\rangle$ and $|d\rangle$ are excited states that decay at rates γ_c and γ_d , respectively. Level $|a\rangle$ is the ground state and $|b\rangle$ is a metastable state with negligible decay rate ($\gamma_b \approx 0$). These levels could be, for example, two hyperfine-split states of an alkaline atom. Levels $|a\rangle$ and $|c\rangle$ are connected by a probe beam with Rabi frequency Ω_p and wavelength λ , while the $|b\rangle \rightarrow |c\rangle$ transition is driven by a coupling beam (Rabi frequency Ω_c). Both coupling and probe beams are resonant with their respective transitions. The signal beam (Ω) is detuned from the $|b\rangle \rightarrow |d\rangle$ transition by $\delta = \omega_{bd} - \omega$, where ω_{bd} is the atomic transition frequency, and ω is the signal optical frequency. We consider a homogeneously broadened medium.

The main element in the atomic model is the Λ type subsystem formed by levels $|a\rangle$, $|b\rangle$, and $|c\rangle$. In the absence of the signal field, if $\gamma_c > \Omega_c \gg \Omega_p$, two indistinguishable pathways to probe absorption are created that interfere destructively. Probe absorption is canceled, and the atomic medium becomes transparent to the probe field [1]. Furthermore, probe transparency is accompanied by an increased steepness in the dispersion around resonance.

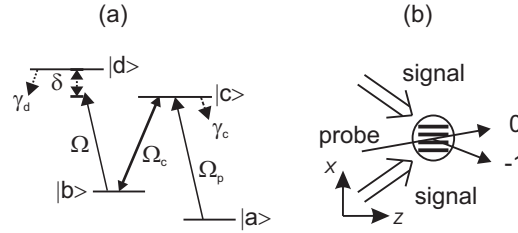


Fig. 1. (a) The atomic model: An open four-level atom interacting with three laser beams: probe (Ω_p), coupling (Ω_c) and signal (Ω). (b) Sketch of the probe- and signal-beam spatial configuration with respect to the atomic sample showing the zeroth and first diffraction orders. The coupling beam (not shown) is parallel to the incident probe beam.

With the signal field present, level $|b\rangle$ suffers an ac-Stark shift, which, because of the steep dispersion, leads to a large change in the index of refraction at the probe frequency [1, 10]. It can be shown that the induced polarization component at the probe frequency ω_p is $P(\omega_p) = \epsilon_0 \chi(\omega_p) E_p(\omega_p)$, where [9, 10]

$$\begin{aligned} \text{Re}[\chi] &= (2N\mu_{ac}^2/\hbar\epsilon_0) \frac{2(\Omega/\Omega_c)^2 \delta}{4\delta^2 + [\gamma_d + \gamma_c(\Omega/\Omega_c)^2]^2}, \\ \text{Im}[\chi] &= (2N\mu_{ac}^2/\hbar\epsilon_0) \frac{\gamma_d(\Omega/\Omega_c)^2 + \gamma_c(\Omega/\Omega_c)^4}{4\delta^2 + [\gamma_d + \gamma_c(\Omega/\Omega_c)^2]^2}. \end{aligned} \quad (1)$$

In deriving Eqs. (1) no approximations were made with respect to the magnitude of Ω , Ω_c or δ . The nonlinear atomic susceptibility χ is a function of two externally controllable parameters: the signal detuning δ and the ratio of signal to coupling Rabi frequencies Ω/Ω_c .

To simplify the notation, we define $\Delta = \delta/\gamma_c$, $R = \Omega/\Omega_c$, and $\Gamma = \gamma_d/\gamma_c$. In the limit of large

signal detunings ($\Delta \gg R, \Gamma$), Eqs. (1) become:

$$\begin{aligned}\operatorname{Re}[\chi] &= A \frac{R^2}{2\Delta}, \\ \operatorname{Im}[\chi] &= A \frac{\Gamma R^2 + R^4}{4\Delta^2},\end{aligned}\quad (2)$$

where $A = 2N\mu_{ac}^2/\gamma_c\hbar\epsilon_0$.

As discussed in Ref. [10], in the limit that $R \ll 1$, this excitation scheme is capable of yielding giant Kerr nonlinearities while keeping the linear susceptibilities identically zero for all fields. The XPM phase shift induced on the probe by the signal field is $\varphi = (\pi\ell/\lambda)\operatorname{Re}[\chi]$, where ℓ is the medium length. The scheme is limited only by the small nonlinear absorption given by $\alpha = (2\pi/\lambda)\operatorname{Im}[\chi]$, and long medium lengths are then possible. Phase shifts of the order of π with single photons in the signal field were proposed. But large nonlinearities at low light levels are also possible for short medium lengths if $R \gtrsim 1$ as was experimentally observed in cold Rb atoms in a magneto-optical trap under this same excitation scheme [15].

If now the signal field is composed of two waves overlapping at the atomic sample at an angle, as shown in Fig. 1b, a standing wave is formed in the x direction. The signal Rabi frequency becomes:

$$\Omega(x) = \Omega \sin(\pi x/\Lambda), \quad (3)$$

where π/Λ is the spatial frequency of the standing wave modulation, which is controlled by the angle at which the two signal beams intersect. Throughout our analysis, we will consider $\Lambda = 4\lambda$, without loss of generality. The signal-to-coupling Rabi frequency ratio R also becomes modulated at this same spatial frequency. As a result, a spatial modulation is introduced to the atomic susceptibility: $\chi = \chi(x)$, creating a grating on which the probe beam can diffract.

Substituting Eqs. (3) into (2), we find

$$\operatorname{Re}[\chi] = A\sigma \sin^2(\pi x/\Lambda), \quad (4)$$

$$\operatorname{Im}[\chi] = A\alpha_2 \sin^2(\pi x/\Lambda) + A\alpha_4 \sin^4(\pi x/\Lambda), \quad (5)$$

where $\sigma = R^2/2\Delta$ is related to the XPM phase shift φ , while $\alpha_2 = \Gamma R^2/4\Delta^2$ and $\alpha_4 = R^4/4\Delta^2$ are related to the nonlinear absorption coefficient α . Both the real and imaginary parts of the susceptibility are modulated by the signal standing wave. Since $\operatorname{Im}[\chi]$ determines the absorption, modulation of $\operatorname{Im}[\chi]$ gives rise to an amplitude grating in the atomic sample. $\operatorname{Re}[\chi]$ is related to the index of refraction, and a modulation in $\operatorname{Re}[\chi]$ generates a phase grating.

3. Coupled wave analysis

To calculate the diffraction efficiency of the EIG, we apply the coupled wave analysis developed for thick hologram gratings by Kogelnik [14]. This analysis considers a monochromatic light incident on the hologram grating at or near the Bragg angle. Similarly to Ref. [14], we write the total probe field inside the atomic grating as the sum of a fundamental mode $S_0(z)$ and a first-order diffracted mode $S_1(z)$:

$$E(x, z) = S_0(z)e^{i\vec{\rho}_0 \cdot \vec{x}} + S_1(z)e^{i\vec{\rho}_1 \cdot \vec{x}}, \quad (6)$$

where $\vec{\rho}_{0,1}$ are the propagation vector of the zeroth (first) diffracted order, respectively. The two waves exchange energy as they propagate inside the atomic sample, and their complex amplitudes $S_{0,1}$ vary along z .

The coordinate axes are defined as shown in Fig. 2a. Both x and z axes are in the plane of incidence and the y -axis is perpendicular to the paper. The grating vector \mathbf{K} is oriented along

the x -axis. Although the signal standing wave is modulated at a spacial frequency equal to π/Λ , the atomic susceptibility (and consequently, the grating) is modulated at twice that frequency as can be seen by making use of the trigonometric identity $\sin^2 u = (1 - \cos 2u)/2$ in Eq. (5). Therefore, the length of the grating vector is $K = 2\pi/\Lambda$. The probe beam enters the grating at an angle θ , with respect to the z axis, at or near Bragg incidence. The probe field is polarized perpendicularly to the plane of incidence, along the y -axis. Figure 2b shows the propagation

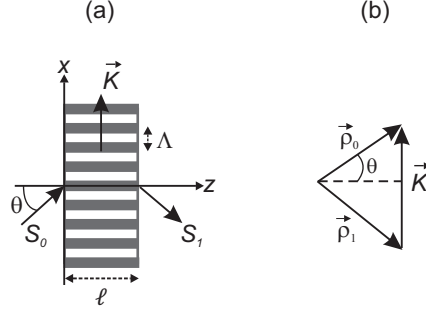


Fig. 2. (a) Illustration of the thick atomic grating showing the probe's angle of incidence θ , the grating vector \vec{K} , the grating period Λ , and the grating thickness ℓ . (b) Vector diagram showing the relation between the zeroth- and first-order propagation vectors and the grating vector.

vectors $\vec{\rho}_{0,1}$, defined as

$$\vec{\rho}_0 = \begin{pmatrix} \rho_{0x} \\ 0 \\ \rho_{0z} \end{pmatrix} = \beta \begin{pmatrix} \sin \theta \\ 0 \\ \cos \theta \end{pmatrix} \quad (7)$$

and

$$\vec{\rho}_1 = \begin{pmatrix} \rho_{1x} \\ 0 \\ \rho_{1z} \end{pmatrix} = \beta \begin{pmatrix} \sin \theta - K/\beta \\ 0 \\ \cos \theta \end{pmatrix}, \quad (8)$$

where $\beta = 2\pi/\lambda$ is the free-propagation wave number. Forced by the grating, the two vectors satisfy

$$\vec{\rho}_1 = \vec{\rho}_0 - \vec{K}. \quad (9)$$

For incidence at the Bragg angle θ_B , where

$$\sin \theta_B = K/2\beta = \lambda/2\Lambda, \quad (10)$$

the length of the two vectors will be equal to the free propagation constant: $\rho_0 = \rho_1 = \beta$. For $\Lambda = 4\lambda$, the Bragg angle is $\theta_B \approx 7.2^\circ$.

Inside the atomic medium, the probe electric field $E(x, z)$ satisfies the scalar wave equation

$$\nabla^2 E + \beta^2(1 + \chi)E = 0. \quad (11)$$

The coupled wave equations for the S_0 and S_1 fields are obtained by substituting Eq. (6) into (11), combined with (9). We then compare terms with equal exponentials ($e^{i\vec{\rho}_0 \cdot \vec{x}}$ and $e^{i\vec{\rho}_1 \cdot \vec{x}}$). Neglecting terms in $\vec{\rho}_0 + \vec{K}$, $\vec{\rho}_1 - \vec{K}$ and the other higher diffraction orders, after much algebra, we find

$$\begin{aligned} S_0'' + 2i\rho_{0z}S_0' + (2\kappa\beta + i\beta\psi_1)S_0 &= (\kappa\beta + i\beta\psi_2)S_1, \\ S_1'' + 2i\rho_{1z}S_1' + [2\kappa\beta + i\beta\psi_1 + (\beta^2 - \rho_1^2)]S_1 &= (\kappa\beta + i\beta\psi_2)S_0, \end{aligned} \quad (12)$$

where $\kappa = \sigma/4z_0$, $\psi_1 = (\alpha_2 + 3\alpha_4/4)/2z_0$ and $\psi_2 = (\alpha_2 + \alpha_4)/4z_0$.

Assuming a slow transfer of energy between the two diffraction orders, the second derivatives in Eqs. (12) can be neglected. And the coupled wave equations become

$$(\cos \theta) S_0' + \alpha_A S_0 = -i\kappa_A S_1, \quad (13)$$

$$(\cos \theta) S_1' + (\alpha_A - i\vartheta) S_1 = -i\kappa_A S_0. \quad (14)$$

where $\kappa_A = (\kappa + i\psi_2)/2$, $\alpha_A = (-2i\kappa + \psi_1)/2$ and $\vartheta = (\beta^2 - \rho_1^2)/2\beta$. The coupling constant κ_A is main parameter in the coupled wave analysis since it couples the propagation dynamics of the two waves. It depends on both the XPM phase shift through σ and the nonlinear absorption through $\alpha_{2,4}$. Because of the coupling, the two waves exchange energy as they propagate inside the grating. In the absence of the signal field ($R = 0$), there is no coupling between S_0 and S_1 ($\kappa_A = 0$), and therefore no diffraction. Changes of wave amplitude because of absorption are related to $\text{Re}[\alpha_A]$, while $\text{Im}[\alpha_A]$ changes the phase of the waves due to XPM between the signal and probe fields. When the incident probe field enters the atomic sample at an angle different from the Bragg angle ($\theta \neq \theta_B$), the diffracted wave S_1 is shifted out of phase with S_0 by an amount proportional to ϑ , thus decreasing the interaction between the two waves. At Bragg incidence $\vartheta = 0$, and the two waves propagate in phase. Our analysis of the atomic phase grating is based on these coupled equations, which govern the propagation of the zeroth and first diffracted orders inside the atomic grating.

Solutions to Eqs. (13) and (14) are of the form

$$S_0(z) = A_0 \exp(\xi_0 z) + B_0 \exp(\xi_1 z), \quad (15)$$

$$S_1(z) = A_1 \exp(\xi_0 z) + B_1 \exp(\xi_1 z), \quad (16)$$

where $A_{0,1}$ and $B_{0,1}$ are constants. Substituting Eqs. (15) and (16) into the coupled wave equations, we obtain the wave numbers

$$\xi_{0,1} = \frac{(i\vartheta - 2\alpha_A) \pm i\sqrt{\vartheta^2 + 4\kappa_A^2}}{2\cos \theta}, \quad (17)$$

with the plus sign corresponding to ξ_0 and the minus sign to ξ_1 .

To determine the constants $A_{0,1}$ and $B_{0,1}$, we need to specify the boundary conditions. We take the amplitude of the incident wave to be unity $S_0(0) = 1$ and that of the diffracted wave to be zero $S_1(0) = 0$ at $z = 0$. From these conditions, we find

$$A_1 = -B_1 = -\frac{\kappa_A}{\sqrt{\vartheta^2 + 4\kappa_A^2}}. \quad (18)$$

At the Bragg angle, $A_1 = -B_1 = -1/2$.

Substituting Eqs. (18) and (17) into (16), we obtain a general expression for the amplitude of the diffracted wave at the output ($z = \ell$) of the atomic sample:

$$S_1(\ell) = -2i \frac{\kappa_A}{\sqrt{\vartheta^2 + 4\kappa_A^2}} e^{i\vartheta\ell/2\cos\theta} e^{-\alpha_A\ell/\cos\theta} \sin \left[\sqrt{\vartheta^2 + 4\kappa_A^2} (\ell/2\cos\theta) \right]. \quad (19)$$

This result is valid for an angle of incidence at or near the Bragg angle. Defining the diffraction efficiency as

$$\eta = S_1 S_1^*, \quad (20)$$

it is straightforward to substitute Eq. (19) into (20) to find η . At Bragg incidence,

$$\eta = \exp[-(\alpha_2 + 3\alpha_4/4)\ell/2z_0 \cos \theta] \left\{ \sin^2[\sigma\ell/8z_0 \cos \theta] + \sinh^2[(\alpha_2 + \alpha_4)\ell/8z_0 \cos \theta] \right\}. \quad (21)$$

Equation (21) is the main result of this paper. In contrast to the approach of Ref. [9], the coupled wave analysis provides an analytical expression for the grating's diffraction efficiency. Equation (21) shows the atomic grating is a lossy mix of a phase and an amplitude gratings. The effect of the phase grating is given by the first term inside the curly braces, which depends on the XPM modulation phase shift through σ . The effect of the amplitude grating is described by the second term, dependent on the nonlinear absorption through α_2 and α_4 . The total diffracted intensity is a simple addition of the intensities diffracted by the phase and the amplitude gratings. The exponential, which depends on the coefficients α_2 and α_4 , is an absorption term that limits the total diffraction efficiency, and it insures that Eq. (21) does not yield an efficiency larger than 1. However, as we will discuss in the next section, the phase grating contribution to diffraction is much larger than the amplitude grating contribution.

By inspecting Eq. (19) it can be seen that the diffracted intensity varies with the angle of incidence θ . Away from the Bragg condition, the diffraction efficiency will be smaller than that given by Eq. (21) by a factor of at least $|\kappa_A/(\vartheta^2 + 4\kappa_A^2)^{1/2}|^2$, where ϑ increases as θ deviates from θ_B .

4. Numerical results and discussion

In what follows, we consider typical atomic parameters for the D2 line of Na at $\lambda = 589$ nm as an example of an atomic system suitable for implementing the EIG under consideration here. In this case, $\gamma_d = \gamma_c = 2\pi \times 9.8$ MHz, $\mu_{ac} = 2.49 \times 10^{-29}$ Cm. We also take $N = 10^{12}$ cm $^{-3}$.

Figure 3 shows the first-order diffraction efficiency $\eta = S_1 S_1^*$ as a function of medium length (grating thickness). The medium length ℓ is given in units of the linear absorption length z_0 . Bragg incidence is assumed, so η is calculated from Eq. (21). The diffraction efficiency varies with the medium length as the signal-probe XPM phase shift changes. For a signal detuning $\Delta = 140$, a peak diffraction efficiency of approximately 70% at $\ell \approx 153z_0$ is predicted. This efficiency is significantly higher than the 30% efficiency reported in the Raman-Nath regime in Ref. [9]. Because the nonlinear absorption decreases faster than the XPM phase shift with signal detuning, increasing Δ to 240 allows a higher peak diffraction efficiency: $\eta \approx 80\%$, at the expense of a longer medium. The small nonlinear absorption prevents the grating from reaching a 100% diffraction efficiency into the first order.

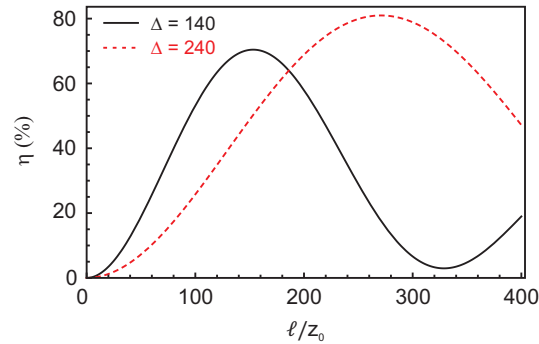


Fig. 3. The diffraction efficiency η as a function of medium length ℓ , in units of z_0 . A signal detuning $\Delta = 140$ corresponds to approximately $2\pi \times 1.4$ GHz in Na. The signal-to-coupling Rabi frequency ratio was set to $R = 4.6$.

We next estimate the individual contributions from the phase and amplitude gratings to the total diffraction efficiency. For $\ell = 153z_0$ and $\Delta = 140$, then $\sigma\ell/8z_0 \cos \theta \approx \pi/2$ and $(\alpha_2 + \alpha_4)\ell/8z_0 \cos \theta \approx 0.12$. As a result, the diffracted intensity from the phase component of the atomic grating is $\exp[-(\alpha_2 + 3\alpha_4/4)L/2z_0 \cos \theta] \sin^2[\sigma\ell/8z_0 \cos \theta] \approx 0.700$, while that of the amplitude component is $\exp[-(\alpha_2 + 3\alpha_4/4)\ell/2z_0 \cos \theta] \sinh^2[(\alpha_2 + \alpha_4)\ell/8z_0 \cos \theta] \approx 0.009$. The small contribution of the latter is because, although the imaginary part of the atomic susceptibility is also spatially modulated, its amplitude is very small. The reason is that $\text{Im}[\chi] \propto 1/\Delta^2$, while $\text{Re}[\chi] \propto 1/\Delta$. For a large enough signal detuning, the contribution of the amplitude modulation can be significantly reduced, while that of the phase modulation is kept relevant, particularly at large ℓ . As we previously pointed out, this atomic grating is mostly a phase grating.

Figure 4a illustrates how the first-order diffraction efficiency depends on the ratio of signal-to-coupling Rabi frequencies R . An optimum ratio appears to exist around $R = 4.6$ that maximizes the diffraction efficiency. A secondary ratio also exists that maximizes the efficiency, but at a much smaller value. A similar result was also observed in the Raman-Nath regime [9]. But the analytical expression for the diffraction efficiency allows us to understand this result. In Fig. 4b, the solid red line shows the modulation component of η [terms within braces in Eq. (21)], while the dashed blue line shows only the absorption component [exponential in Eq. (21)]. The diffraction efficiency plot in Figure 4a is obtained by multiplying the two curves in Fig. 4b. Without absorption, there are several values of R for which $\sigma L/8z_0 \cos \theta = m\pi/2$ (where $m = 1, 3, 5, \dots$) and that maximizes η . The non-sinusoidal shape of the curve is due to the R^2 dependence of σ . But absorption of the probe beam (both zeroth and first order waves) also increases with R . This is because if the signal field becomes too strong with respect to the coupling field, the atom is shifted out of the EIT condition, causing it to absorb the probe beam. At $R \approx 4.6$, the signal beam is such that it optimizes the XMP phase shift to maximize diffraction without introducing a significant amount of absorption. But at $R \approx 8$, when the second maximum in the diffraction efficiency occurs, absorption is severe, limiting the efficiency.

In order for EIT to occur, the coupling field must satisfy $|\Omega_c|^2 > \gamma_c \gamma_b$. In the limit that the ground state decoherence $\gamma_b \approx 0$, the coupling field can be made arbitrarily weak. From the results shown above, $\Omega \gtrsim \Omega_c$. So the atomic phase grating can be created with very weak signal fields. In a real atomic sample, such as those in a magneto-optical trap, $\gamma_b \approx 2\pi \times 1$ KHz. Therefore, a grating created with a signal field with Rabi frequency $\Omega > 2\pi \times 455$ KHz, will efficiently diffract a weak probe beam. This signal level is well below saturation level and even below the typical linewidth of lasers used in many EIT experiments, which would ultimately limit Ω .

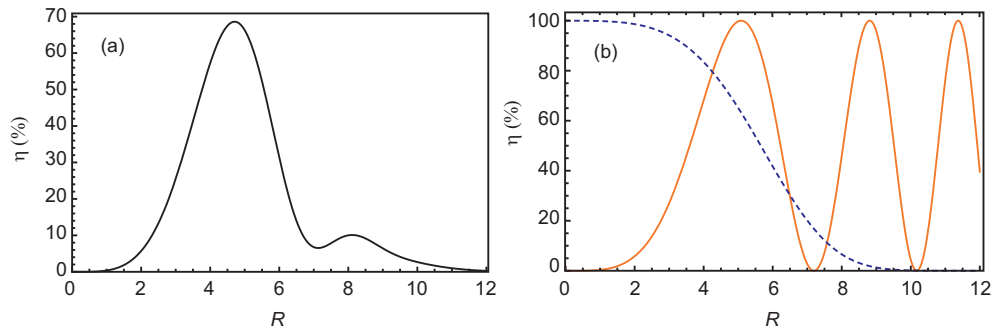


Fig. 4. (a) The first-order diffraction efficiency η as a function of the ratio of signal-to-coupling Rabi frequencies R for $\ell = 135z_0$, $\Delta = 140\gamma_c$. (b) Absorption (dashed blue line) and modulation (solid red line) components of η as a function of R .

And finally, we investigated how the diffraction efficiency depends on the angle of incidence. Figure 5 shows the efficiency of the atomic grating as a function of angular deviation $\Delta\theta \equiv \theta_B - \theta$ from the Bragg angle. It is seen that the grating is very sensitive to the angle of incidence; with a deviation of less than 2 mrad from Bragg incidence, the efficiency drops to half its value at Bragg angle. From [14], the acceptance angle (full width at half maximum) of a thick grating can be estimated as $2\Delta\theta \approx \Lambda/\ell$. Because our grating thickness ℓ is very much larger than its period Λ , its acceptance angle is very small. However, the angle between the two signal beams that form the atomic grating may be adjusted to increase the grating period, increasing the acceptance angle. The Bragg angle will decrease, but because $\cos \theta_B \approx 1$, the diffraction efficiency [Eq.(21)] will not be affected.

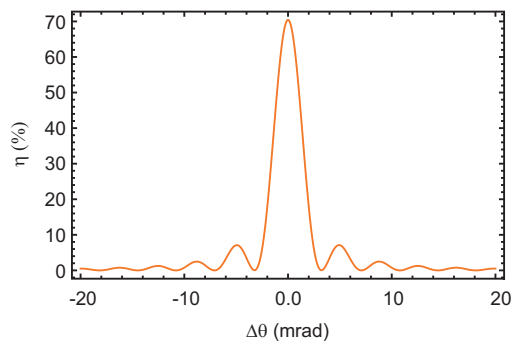


Fig. 5. Diffraction efficiency η as a function of angular deviation $\Delta\theta$ from Bragg incidence. Here, $R = 4.6$, $\Delta = 140$ and $\ell = 153z_0$.

5. Conclusion

We investigated theoretically the properties of an electromagnetically-induced phase grating by means of a coupled-wave theory analysis. The phase grating relies on the giant Kerr nonlinearity an atom experiences under electromagnetically induced transparency. We derived an analytical expression for the diffraction efficiency of the grating and showed that high diffraction efficiencies ($> 70\%$) of a resonant probe beam are possible. The large efficiencies are obtained for Bragg incidence of the probe beam, and the diffraction efficiency decreases rapidly with angular deviations from the Bragg angle.

To obtain the large diffraction efficiencies predicted in the theory, large optical depths (> 150) are required. Such optical depths are easily obtained in atomic vapor cells, although the effect of Doppler broadening would need to be included in the model for more precise predictions. We note, however, that our model can be applied to those cells in which the atomic density is so high that the transitions become homogeneously broadened by collisions. Optical depths as high as 160 have been observed experimentally in “dark-spot” sodium magneto-optical traps [16], and optical depths approaching 300 in cold atomic Rb samples have been recently produced by combining rapid, high-flow vapor injection with buffer gas cooling [17]. So the grating described here can be implemented with existing technology.

Acknowledgements

This work was financially supported by FAPESP and INOF-CNPq. The authors thank Jaime F. Sochaczewsky for pointing out that the atomic grating might be thick.